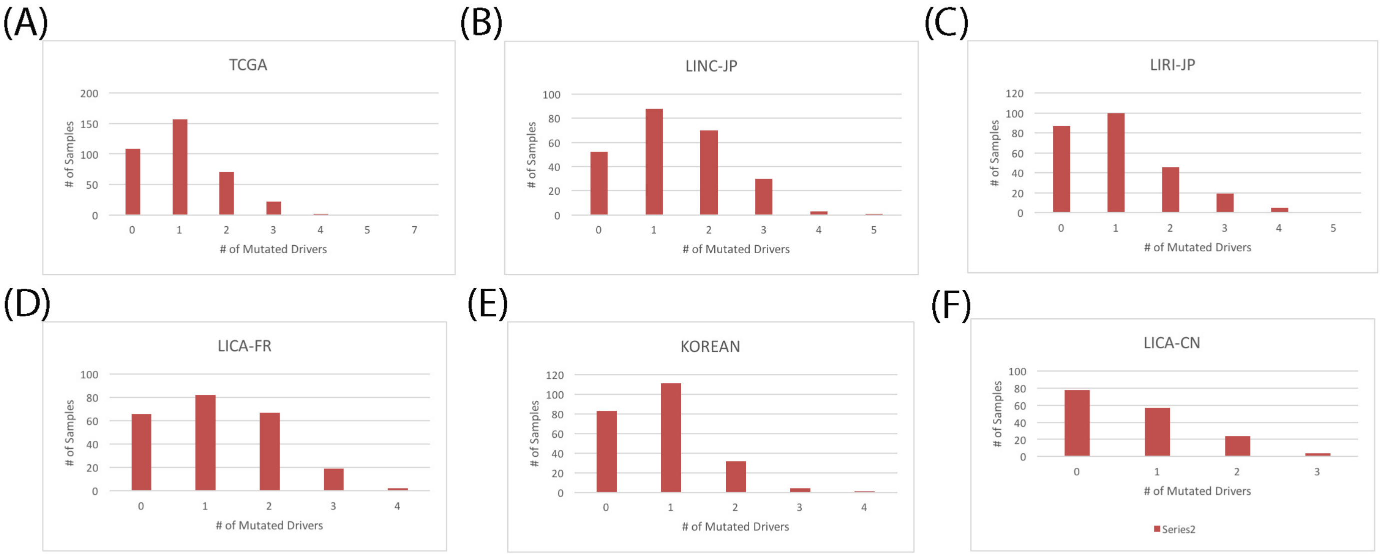

Supplementary Figure S1: Distributions of the number of mutated consensus drivers in the six cohorts.

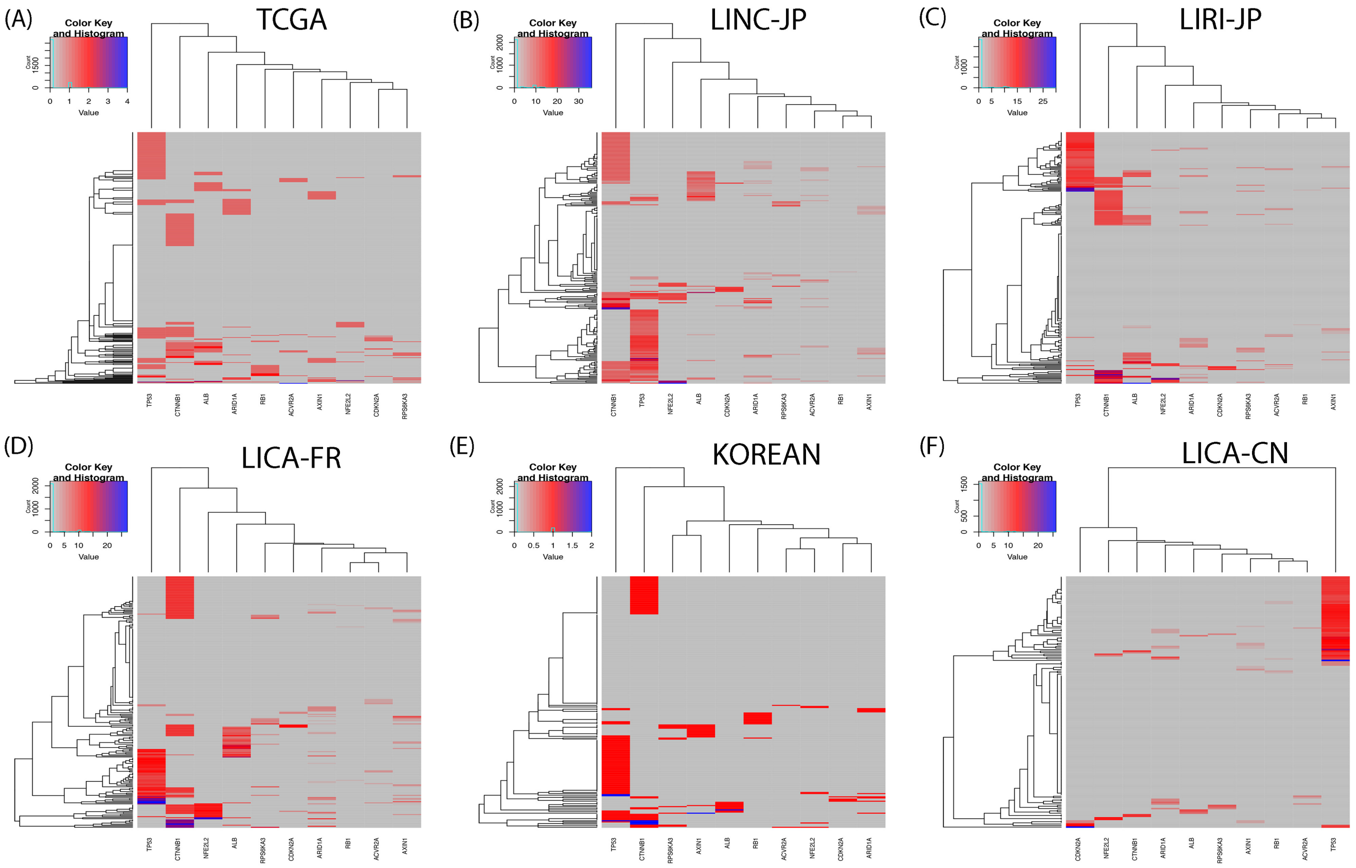

Supplementary Figure S2: Heatmaps of mutation counts in consensus drivers across samples in the six cohorts. Red and blue colors represent low and high mutation counts in a particular driver.

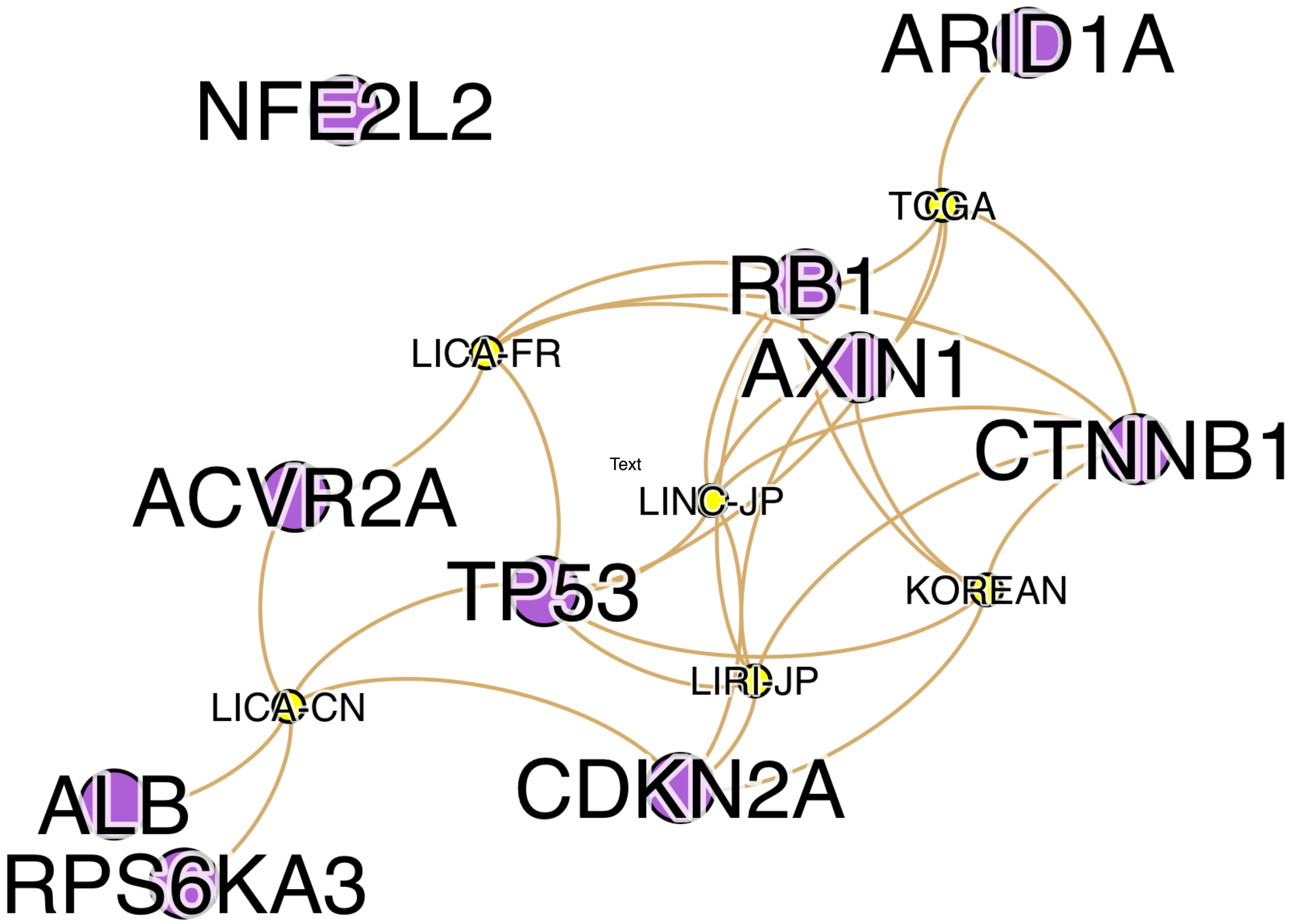

Supplementary Figure S3: Bipartite graph showing the distribution of mutually exclusive genes identified with Dendrix across the 6 cohorts. Purple and yellow nodes represent genes and cohorts, respectively where the size of the node is proportional to the connectivity.

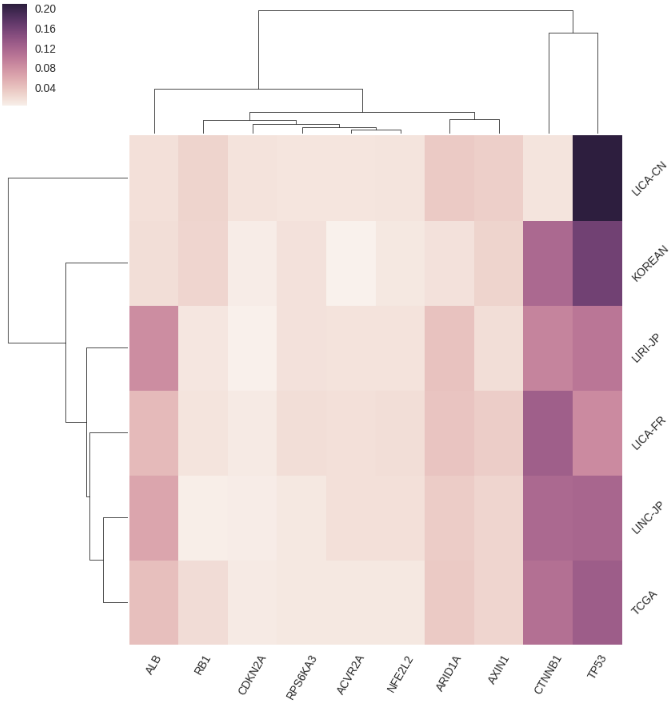

Supplementary Figure S4: Similarity of the bipartite graphs among HCC cohorts based on pageRank scores. The darker color represents more predominant mutations.

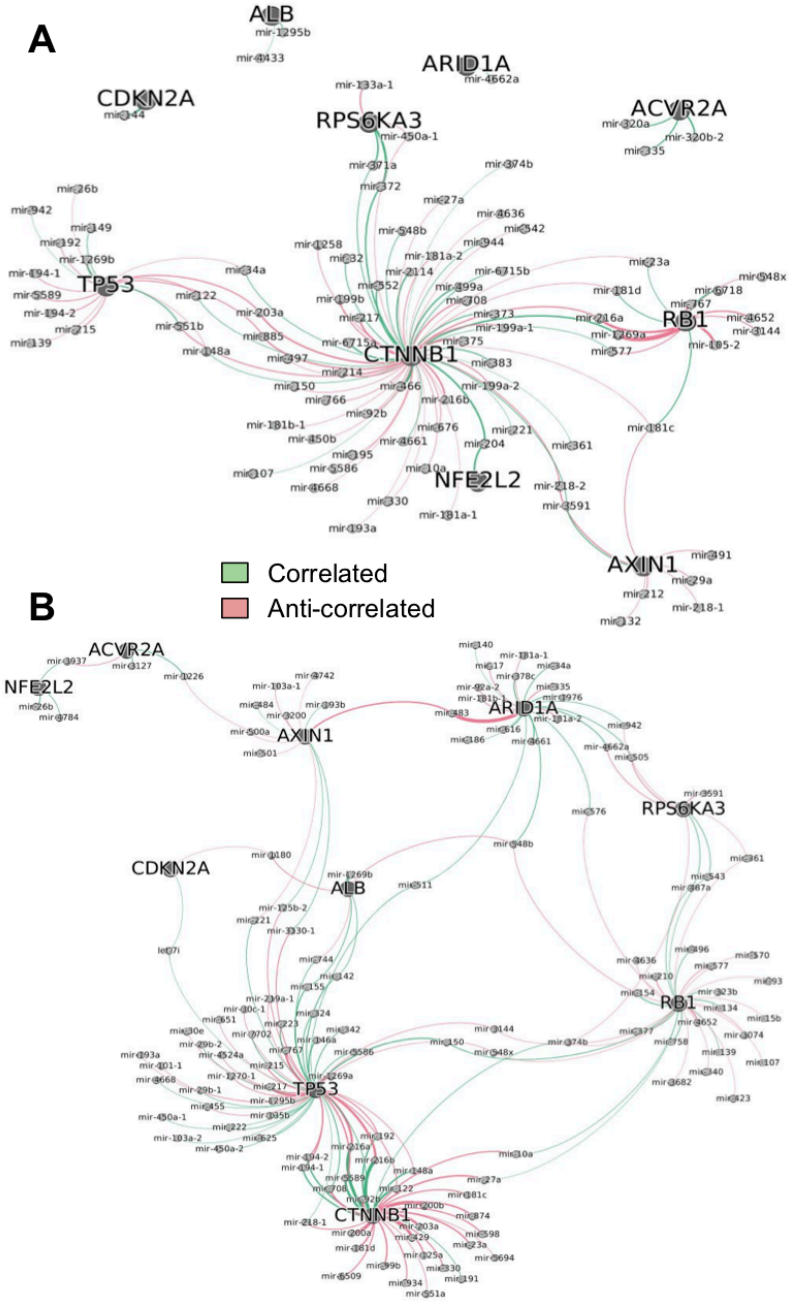

Supplementary Figure S5: Associations of consensus driver genes with miR expression. Bipartite graphs representing (A) correlations between miR expression and mutations of the genes. (B) Correlations between miR expression and CNV. Green color represents positive correlation and red for anti-correlation.

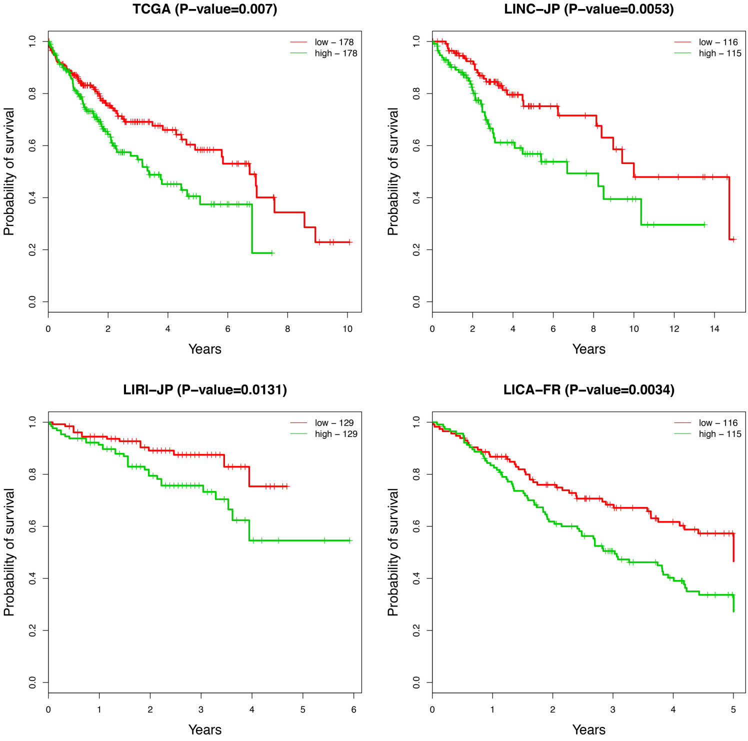

TCGA (P–value=0.007)

LINC–JP (P–value=0.0053)

LIRI–JP (P–value=0.0131)

LICA–FR (P–value=0.0034)

Supplementary Figure S6: Kaplan-Meier estimates of overall survival (OS) in 4 HCC cohorts. A Cox-PH regression was used to build the overall survival model featuring the driver genes mutation profile. The samples were dichotomized into high and low risk groups by the median Prognostic Index (PI). (A) TCGA (B) LINC-JP (C) LIRI-JP (D) LICA-FR cohorts.

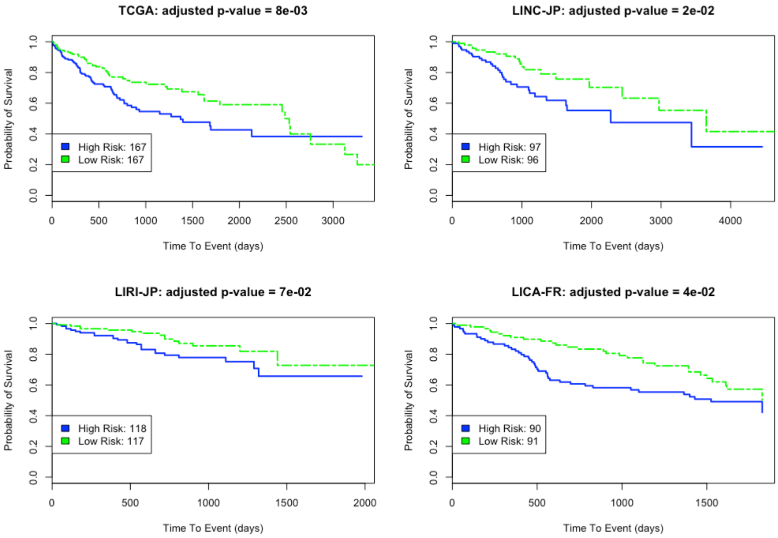

Supplementary Figure S7: Kaplan-Meier of overall survival (OS) after adjustment for gender, age, stage, and grade. (A) TCGA (B) LINC-JP (C) LIRI-JP (D) LICA-FR cohorts.

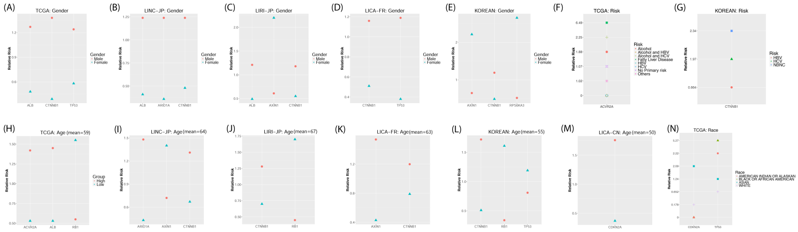

Supplementary Figure S8: Associations of gender and age with driver genes. Shown are subsets of consensus driver genes with significant associations with gender (Fisher's exact test with p-value<0.05) or age (Mann-Whitney-Wilcoxon test with p-value<0.05). Age is divided to two groups by the mean value (in parentheses) in each cohort.